Nonlinear Two-Dimensional Unsteady Potential Flow with Lift

JOSEPH P. GIESING*
Douglas Aircraft Company, Long Beach, Calif.

A method has been developed for calculating the pressure, forces, and moments on a two-dimensional airfoil of arbitrary shape executing arbitrary unsteady motions. The fluid medium through which the airfoil moves is assumed to be inviscid and incompressible. The vortex-sheet wake shed by the airfoil is carried along by the fluid particles to which it is attached and changes in shape with time. The method makes no assumptions as to the type or amplitude of motion and is limited only by the storage of the IBM 7094 computer that carries out the calculations. Pressure calculations are shown for airfoils executing periodic and transient motions. Wake shapes for such motions are also shown. In addition, the method is compared with experimental data and other theoretical methods. Finally, a study that shows the effects of nonlinearity on the Theodorsen, Wagner, and Küssner functions is presented. Nonlinear effects are due to airfoil thickness, amplitude of motion, frequency of oscillation, and gust magnitude.

Nomenclature

C = Theodorsen function
c = position of wake element; also chord length
$\hat{C}_l$ = lift coefficient (less the added-mass terms proportional to accelerations) divided by quarter-chord amplitude
$\hat{C}_m$ = moment coefficient analogous to $\hat{C}_l$
F = potential due to unit sources located at the intersection of airfoil surface and gust edge
G = potential due to a unit point vortex
$\mathbf{i}, \mathbf{j}$ = unit vectors in the x and y directions
K = circulation about an airfoil due to its immersion in the flowfield of a point vortex
k = nondimensional half frequency, $\omega/2$
$\mathbf{n}, \mathbf{t}$ = unit vectors in the normal and tangential directions
$\mathbf{R}$ = position vector from a fixed inertial point to a vortex-wake element
r = position vector from the origin, in airfoil coordinates, to a general field point
t = time
U_∞ = arbitrary normalizing velocity
$\mathbf{V}$ = disturbance velocity
$\mathbf{V}_f$ = velocity of the airfoil
x, y = Cartesian coordinates fixed in airfoil
Γ = airfoil circulation
γ = wake-element vorticity strength
Φ = Wagner function
φ = disturbance potential
ψ = Küssner function
Ω = angular velocity
ω = nondimensional frequency, (frequency) c/U_∞

Subscripts

D = the part of the wake generated up to time t_1 considered at time $t_1 + \Delta t$
d = disturbance potential and circulation due to entire wake
G = gust onset flow
g = gust disturbance flow
Q = quasi-steady flow
w = wake
x, y = x and y components
Γ = circulatory flow
0 = angle of attack of 0°
90 = angle of attack of 90°

Presented as Paper 66-968 at the AIAA Third Annual Meeting, Boston, Mass., November 29–December 2, 1966; submitted August 7, 1967; revision received November 17, 1967. This research was carried out under the Bureau of Ships Fundamental Hydromechanics Research program, NS 715-102, administered by the David Taylor Model Basin. The author wishes to acknowledge the assistance of K. Haynes and K. Tsurasaki of the Douglas Scientific Computer Programming Group.

* Scientist-Specialist, Aerodynamics Research Group, Aircraft Division.

Introduction

THE potential-flow theory for thin plates executing small-amplitude, simple-harmonic motions has been presented by Karman and Sears[1] and Theodorsen.[2] The theory of transient motions of flat plates has been developed by Wagner[3] and Küssner.[4] The effects of thickness of airfoils in small-amplitude, simple-harmonic motion has been studied recently by Küssner,[5] Van De Vooren,[6] and Hewson-Brown.[7] For practical calculations using these last three methods, the circle-airfoil conformal mapping must not only be known but should be simple. Only Van De Vooren has produced an actual pressure distribution.

It is of interest to know to what extent these approximate theories may be applied to nonlinear problems and to know how to obtain a solution if they fail to apply. The effect of viscosity, which has never been successfully treated, is also of interest. Before a theory for the effect of viscosity can be developed, methods for predicting pressure distributions on airfoils in unsteady motions must be available. This is true because boundary-layer characteristics are a direct function of the pressure distribution. If empirical methods are sought, it is of importance to isolate the viscous effects from the nonlinear effects. This can be done only if the nonlinear effect are fully known.

A general nonlinear potential-flow theory that includes the determination of the airfoil pressure distribution is needed. Such a method has been developed and is presented here.

The nonlinear unsteady potential-flow problem is solved with the aid of a very general and powerful method developed by Smith,[8] Hess,[9] and Giesing[10] for the steady potential-flow problem. This method is applied step by step in time, starting from a given initial airfoil position and orientation and proceeding step by step along the airfoil flight path. A detailed description of the method is given by Giesing.[11, 12] The present method is limited only by the storage of the computer that carries out the calculations. This limitation fixes the maximum number of steps at 100 for the IBM 7094. The airfoil shape, which may be arbitrary, is put in to the computer as a series of coordinates. The maximum number of defining coordinates is also limited to 100.

Unlike all previous theories, there exists the possibility of extending the present method to include more than one body. Such an extension to the case of two bodies (two airfoils, an

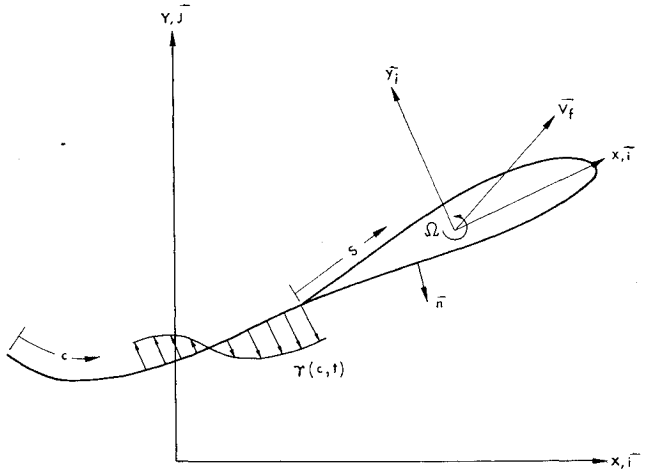

Fig. 1 Coordinate system for the airfoil and wake.

airfoil and a nonlifting body, etc.) is in the process of development and will be reported at a later date.

Theory

Problem

It is desired to find the pressure, forces, and moments acting on an airfoil section operating unsteadily in an incompressible inviscid fluid. No restrictions will be placed on the airfoil shape or motion. The solution will be effected by using the two-dimensional, potential-flow model. Therefore, the basic equations governing the fluid motion and pressure are the Laplace and Bernoulli equations, respectively. In addition, the continuity of vorticity must be preserved. Any loss of circulation must show up in the wake as shed vorticity. Since the flow will be determined with reference to a coordinate system fixed in the airfoil, the Bernoulli equation must be written for a translating and rotating frame of reference.[13] If V_f and Ω are the translational and rotational speeds of the airfoil, respectively (see Fig. 1) and $\mathbf{V}$ is the gradient of the disturbance potential ($\mathbf{V} = \nabla\varphi$), then the Bernoulli equation is written as follows:

$$C_p = \frac{p - p_\infty}{\frac{1}{2}\rho U_\infty^2} = \left(\frac{V_s}{U_\infty}\right)^2 - \left(\frac{V_T}{U_\infty}\right)^2 - \frac{2}{U_\infty^2}\frac{\partial\varphi}{\partial t} \qquad (1)$$

where $\mathbf{V}_s = \mathbf{V}_f + \Omega(\mathbf{j}x - \mathbf{i}y)$; $\mathbf{V}_T = \nabla\varphi - \mathbf{V}_s$; and U_∞ is an arbitrary reference speed.

The general boundary condition for the problem is simply that the fluid not penetrate the airfoil surface. The total velocity of the fluid, $\mathbf{V}_T$, as viewed in the moving airfoil coordinate system, cannot have a component normal to the airfoil surface S, that is, $\mathbf{V}_T \cdot \mathbf{n} = 0$. Upon using the definition of $\mathbf{V}_T$, the boundary condition for the disturbance potential φ may be determined as

$$\partial\varphi/\partial n = \mathbf{V}_s \cdot \mathbf{n} \qquad \text{on } S \qquad (2)$$

The specific problem posed is, then, to find the disturbance potential φ caused by an airfoil moving unsteadily through the fluid and shedding vorticity of unknown strength. The problem also involves finding the shed-vorticity strength, airfoil circulation, and vortex-wake position and motion.

Solution for the Potential

It will facilitate the solution if the potential φ is split into two major parts, one due to quasi-steady motion (motion neglecting airfoil circulation and wake) and one due to the circulation and wake alone. The quasi-steady potential φ_Q is a function only of the airfoil instantaneous translational and angular velocity and may be parameterized by them. Specifically,

$$\varphi_Q(r,t) = U_x(t)\varphi_0(r) + U_y(t)\varphi_{90}(r) + \Omega(t)\varphi_\Omega(r) \qquad (3)$$

where φ_0, φ_{90}, and φ_Ω are the component disturbance potentials due to flows of unit strength at 0° and 90° angle of attack and unit rotational speed, respectively. The speeds U_x, U_y, and Ω are the components of the onset flows $-\mathbf{V}_s$ in the horizontal, vertical, and angular directions, respectively. Specifically,

$$-\mathbf{V}_s = \mathbf{i}U_x + \mathbf{j}U_y + \Omega(\mathbf{i}y - \mathbf{j}x)$$

where it is assumed that U_x and U_y are in the positive x and y directions, respectively, and that Ω is positive counterclockwise. Unlike U_x, U_y, and Ω, the component potentials φ_0, φ_{90}, and φ_Ω are not functions of time, and thus may be found once and for all. The boundary conditions applied at the airfoil surface S for these potentials are

$$\partial\varphi_0/\partial n = \mathbf{i}\cdot\mathbf{n} \qquad \partial\varphi_{90}/\partial n = \mathbf{j}\cdot\mathbf{n} \qquad \text{on } S$$
$$\partial\varphi_\Omega/\partial n = (\mathbf{i}y - \mathbf{j}x)\cdot\mathbf{n} \qquad \text{on } S \qquad (4)$$

The second part of the potential φ (potential due to circulation and wake alone) will be termed φ_w; the boundary condition for it is homogeneous;

$$\partial\varphi_w/\partial n = 0 \qquad \text{on } S \qquad (5)$$

This simply means that the disturbance flow caused by the wake and circulation may not penetrate the airfoil surface. It is convenient to split φ_w into several components as φ_Q was split. The flow represented by the potential φ_w may be thought of as a flow due to a vortex sheet alone (φ_s) plus a flow (φ_d) necessary to satisfy the airfoil boundary condition (5) plus a pure circulatory flow ($\Gamma\varphi_\Gamma$). Thus,

$$\varphi_w(r,t) = \varphi_s(r,t) + \varphi_d(r,t) + \Gamma(t)\varphi_\Gamma(r) \qquad (6)$$

The boundary conditions for the individual terms are

$$\partial\varphi_d/\partial n = -\partial\varphi_s/\partial n \qquad \text{on } S \qquad (7a)$$

$$\partial\varphi_\Gamma/\partial n = 0 \qquad \text{on } S \qquad (7b)$$

The flow generated by the wake vortex sheet (whose potential is φ_s) is assumed to be known. The value of φ_s on the airfoil surface S is obtained by integrating the effects of the wake-vortex elements;

$$\varphi_s = \int_w G(c,t)\gamma(c)dc \qquad (8)$$

where w stands for integration over all the wake-vortex elements. The term $G(c,t)\gamma(c)$ is the potential due to an elemental vortex of strength γ in the wake. Figure 1 shows a schematic of the airfoil and wake with the associated coordinate systems.

The boundary conditions for all the unknown component disturbance potentials are now known, being given by Eqs. (4) and (7). It remains to find the potential fields that correspond to these boundary conditions.

Potential-Flow Operator

A method is sought that will produce φ when $\partial\varphi/\partial n$ is known. Such a method could be used to find φ_0, φ_{90}, φ_Ω, and φ_Γ once, since they are not functions of time and could be used to find φ_d at every instant of interest. Methods developed by Smith,[8] Hess,[9] and Giesing[10] may be applied directly to this problem. A brief outline of these methods, along with the presentation of the results, will be sufficient for present purposes.

The potential of the flow due to an elementary source satisfies the Laplace equation. The methods of Refs. 8–10 generate the desired disturbance flow φ by superimposing the fields of a distribution of sources. In particular, a continuous distribution is applied to the surface of the body and the

strength of the distribution adjusted in such a way that the resulting velocity field satisfies the prescribed boundary condition on the body surface, i.e., the velocity distribution normal to the body surface ($\partial\varphi/\partial n$) is prescribed. The surface-source strength $\sigma(s)$ is found by solving a Fredholm integral equation of the second kind. The left-hand side of the equation is just the boundary-value distribution, $\partial\varphi/\partial n$. In practice, the body surface is broken up into many short, straight-line elements, over each of which the source strength may be considered to be of constant strength.† The boundary condition on the surface (prescribed $\partial\varphi/\partial n$) is made to hold at the midpoint of each of the elements. The end result is a set of N equations (N is the number of elements) and N unknowns. The unknowns are the N source densities σ_k. These equations may be presented as

$$A_{jk}\sigma_k = (\partial\varphi/\partial n)_j \tag{9}$$

where j ranges over the element midpoints and is just the surface arc-length index. The matrix A_{jk} represents the velocity normal to element j due to element k, which is of unit source strength (see Ref. 10). If H_{lj} and ∇H_{lj} represent the potential and velocity, respectively, at the point r_l due to the jth element, which is of unit source strength, the effect of all the elements at the point r_l is just the sum of the effects; that is,

$$\varphi_l = H_{lj}\sigma_j \tag{10a}$$

and

$$\mathbf{V}_l = \nabla\varphi_l = \nabla H_{lj}\sigma_j \tag{10b}$$

where the point r_l may range over points on the body surface or points out in the flowfield. Equations (9) and (10) may each be combined into one equation as follows:

$$\varphi_l = H_{lq}A_{qp}^{-1}(\partial\varphi/\partial n)_p \tag{11a}$$

$$\mathbf{V}_l = \nabla H_{lq}A_{qp}^{-1}(\partial\varphi/\partial n)_p \tag{11b}$$

The matrices $H_{lq}A_{qp}^{-1}$ and $\nabla H_{lq}A_{qp}^{-1}$ may be thought of as operators, taking $\partial\varphi/\partial n$ and producing φ and $\mathbf{V}$, respectively. Let $H_{lq}A_{qp}^{-1}$ be termed the potential operator PO_{lp} and $\nabla H_{lq}A_{qp}^{-1}$ the velocity operator ΔPO_{lp}. These operators are not functions of time, but are functions only of the airfoil shape and the field points r_l. The operators PO_{lp} and ∇PO_{lp} can be generalized symbolically to the continuous case [input $\partial\varphi/\partial n$, output $\varphi(r)$], keeping in mind that whenever they are to be actually calculated the discrete form is to be used. Such a generalization gives

$$\varphi = PO(\partial\varphi/\partial n) \tag{12a}$$

$$\mathbf{V} = \nabla PO(\partial\varphi/\partial n) \tag{12b}$$

The required time derivative of φ is given by the following:

$$\partial\varphi/\partial t = PO[\partial/\partial n(\partial\varphi/\partial t)] \tag{12c}$$

The time derivative does not interact with the operator, since it is independent of time.

The special case of $\partial\varphi_\Gamma/\partial n = 0$ (pure circulation) must be handled in an indirect manner. The potential φ_Γ is split into two parts, one due to an arbitrary distribution of vorticity within the airfoil (of total strength unity), which is to be considered known, and a disturbance potential needed to make the two together satisfy the homogeneous boundary condition. If these two parts are termed φ_{Γ_1} (internal vorticity potential) and φ_{Γ_2} (disturbance potential), the homogeneous boundary condition for φ_Γ is $\partial(\varphi_{\Gamma_1} + \varphi_{\Gamma_2})/\partial n = 0$, and thus the boundary condition for φ_{Γ_2} is

$$\partial\varphi_{\Gamma_2}/\partial n = -\partial\varphi_{\Gamma_1}/\partial n \qquad \text{on } S$$

† In the method of Ref. 10 the maximum number of describing elements is 500. In the present analysis the maximum number is 100.

The potential operator (12a) may be applied to $\partial\varphi_{\Gamma_2}/\partial n$ to produce φ_{Γ_2}. The two potentials φ_{Γ_1} and φ_{Γ_2} may then be added together to produce φ_Γ.

Strength of Shed Vorticity

In the last section, methods for obtaining the potential field φ, given its normal-derivative boundary conditions $\partial\varphi/\partial n$, were presented. The potential φ_s and thus the boundary condition for φ_d, however, are dependent on the strength γ of the vorticity in the wake and also on the wake position. The airfoil circulation Γ, which is needed to find part of the velocity field, is also dependent on the vorticity strength and wake position. This section describes the procedure for determining the wake vorticity strength.

The Kutta condition requires that the velocities at the trailing-edge upper surface and lower surface be equal in magnitude but opposite in tangential direction. In most cases this is equivalent to requiring that the flow stagnate at the trailing edge.‡ Noncirculatory potential flows usually do not satisfy this condition, and, therefore, a circulatory flow must be added. The strength of the circulatory flow Γ is adjusted until the Kutta condition is satisfied. Once a noncirculatory flow is known, the circulation needed to satisfy the Kutta condition for that flow can easily be obtained. In fact, it is convenient to associate a circulation with each of the noncirculatory flows discussed so far. The total circulation is then the sum of all its components. Specificially, if Γ_0, Γ_{90}, Γ_Ω, and Γ_d are the circulations associated with φ_0, φ_{90}, φ_Ω, and φ_d, respectively, the sum is $\Gamma(t) = U_x(t)\Gamma_0 + U_y(t)\Gamma_{90} + \Omega(t)\Gamma_\Omega + \Gamma_d(t)$;

$$\Gamma = \Gamma_Q + \Gamma_d \tag{13}$$

The first term is the circulation due to the quasi-steady flow found once and for all, and Γ_d is the circulation due to the wake flow. The wake-flow circulation can be expressed as an integral that is analogous to its corresponding potential φ_d;

$$\Gamma_d = \int_w \gamma(c)K(c,t)dc \tag{14}$$

Here $K(c,t)$ is the circulation around the airfoil caused by the immersion of the airfoil in the flowfield of a point unit vortex located at the position c in the wake.

Because the total vorticity of the system is preserved, the sum of the airfoil circulation and the total vorticity in the wake remains constant (for simplicity, set this constant to 0);

$$\Gamma + \int_w \gamma(c)dc = 0 \tag{15}$$

Combining (13–15) gives

$$-\Gamma_Q = \int_w \gamma(c)[1 + K(c,t)]dc \tag{16}$$

This is an integral equation for the unknown vorticity strength $\gamma(c)$, which may be solved in a step-by-step fashion in the following way. Consider that the wake vorticity $\gamma(c)$ is known up to time t_1 (this is general, since t_1 may correspond to the inception of motion). In Eq. (16), the range of integration at time $t_1 + \Delta t$ may then be split into two parts, one part $w(t_1)$ where the vorticity is known and one part $\Delta w = w(t_1 + \Delta t) - w(t_1)$ where the vorticity is unknown. Because of this split, the circulation Γ_d and corresponding potential φ_d must also be split;

$$\Gamma_d = \Gamma_D + \bar{\gamma}\bar{K}\Delta w \tag{17a}$$

$$\varphi_d = \varphi_D + \bar{\gamma}\varphi_K\Delta w \tag{17b}$$

where

$$\Gamma_D = \int_{w(t_1)} \gamma(c)K(c,t_1 + \Delta t)dc \tag{17c}$$

The bar indicates an average over the wake length Δw. The potentials φ_D and φ_K are obtained by first splitting the boundary condition for φ_d and then applying the potential-

‡ Exceptions are cusped trailing edges.

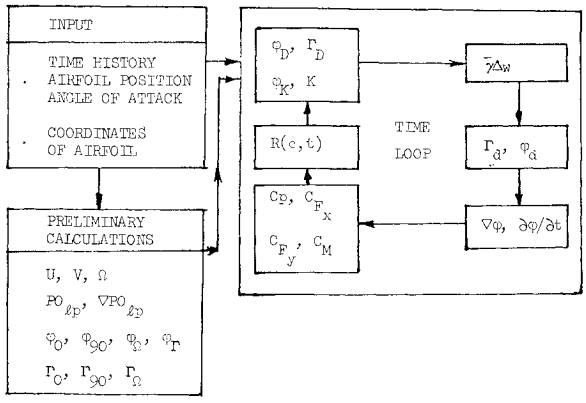

Fig. 2 Flow diagram for the computer program of the present method.

flow operator to both pieces. Once φ_D and φ_K are known (also $\nabla\varphi_D$ and $\nabla\varphi_K$), the circulations Γ_D and $\bar{K}$ can be found. The boundary conditions for φ_D and φ_K, which are obtained from Eqs. (7a) and (8), are

$$\partial\varphi_D/\partial n = -\int_{w(t_1)}\partial G/\partial n\gamma(c)dc \tag{18a}$$

$$\partial\varphi_K/\partial n = -\partial G(\bar{c}_{TE}, t)/\partial n \tag{18b}$$

where $\bar{c}_{TE}$ is a position on the wake near the trailing edge midway between $w(t_1)$ and $w(t_1) + \Delta w$. The term $G(\bar{c}_{TE}, t)$ is just the onset potential due to a point vortex located at $\bar{c}_{TE}$, and φ_K is the corresponding disturbance potential. Since the segment of wake being shed is represented by a point vortex, it is consistent to represent all wake elements as point vortices. Because of this, all integrals become finite sums. Equation (16) may now be solved for $\bar{\gamma}\Delta w$ in terms of Γ_Q, Γ_D, $\bar{K}$ and $\int_{w(t_1)}\gamma(c)dc$ [which is just $\Gamma(t_1)$], as follows:

$$\bar{\gamma}\Delta w(t_1 + \Delta t) = \frac{-\Gamma_Q(t_1 + \Delta t) - \Gamma(t_1) - \Gamma_D(t_1 + \Delta t)}{1 + \bar{K}(t_1 + \Delta t)} \tag{19}$$

The solution for the shed vorticity is now complete, and the solutions for φ_d and Γ_d may be obtained. The addition of the two components of φ_d [Eq. (17b)] can now be effected, since $\bar{\gamma}\Delta w$ is known. The circulation Γ_d can be found by using Eq. (17a). All potentials and circulations are now known and the pressure, forces, and moments can be calculated. It was assumed, however, that the wake shape was known at time t_1, and if we wish to continue the solution beyond $t_1 + \Delta t$, the wake shape as it is at $t_1 + \Delta t$ must be found. The motion of the wake is the subject of the next section.

Motion of Trailing Vortex Sheet

The movement of the trailing vortex sheet is given by the movement of all the vortex particles that compose the sheet. The wake-vortex particles move with the fluid as if they were fluid particles. The trajectory of each particle is obtained by using a simple predictor-corrector integration procedure. If $\mathbf{R}(c, t)$ is the radius vector from a stationary inertial point to the vortex located at c along the wake at the time t, the integration procedure can be written as

$$\mathbf{R}_p = \mathbf{R}(t_1) + \Delta t\mathbf{V}[R(t_1)] \qquad \text{predictor} \tag{20a}$$

$$\mathbf{R}(t_1 + \Delta t) = \mathbf{R}(t_1) + (\Delta t/2)[\mathbf{V}[R(t_1)] + \mathbf{V}(R_p)] \qquad \text{corrector} \tag{20b}$$

where $\mathbf{R}(t_1 + \Delta t)$ is the final result. Equation (20a) is first applied to all the vortex points, after which (20b) is applied to all the points. The disturbance velocity $\mathbf{V} = \nabla\varphi$ is known at time $t_1 + \Delta t$, once $\bar{\gamma}\Delta w$ is known. Thus the wake motion calculation must be carried out after $\bar{\gamma}\Delta w$ is found.

At this point it may be helpful to show the order in which the entire calculation is carried out. Figure 2 gives a schematic diagram of this order. As is shown, the preliminary calculation involving the quasi-steady quantities plus φ_Γ is done once and for all. The only quantities that must be recalculated at each time step are φ_d and Γ_d. The results of these calculations are φ and its time and space derivatives, which are used in the Bernoulli equation to find the pressure. The calculation of pressures, as well as the resulting forces and moments, is described in the next section.

Pressure, Forces, and Moments

In the expression for the pressure coefficient given by Eq. (1), the following three quantities are needed: $\mathbf{V}_s$, $\mathbf{V}_T$, and $\partial\varphi/\partial t$. Since $\mathbf{V}_T$ is just $\mathbf{V} - \mathbf{V}_s$ and since $\mathbf{V}_s$ is determined by the given motion of the airfoil, only $\mathbf{V} = \nabla\varphi$ and $\partial\varphi/\partial t$ need be found. The gradient of the potential φ, i.e., $\mathbf{V}$ has been obtained by using ∇PO for the component parts of φ in the last several sections, and thus only the time derivative of the potential is left to be determined. Finding $\partial\varphi/\partial t$ will be the main objective of this section.

As is noted in Eqs. (3) and (6), the component parts of φ are $U_x(t)\varphi_0 + U_y(t)\varphi_{90} + \Omega(t)\varphi_\Omega + \varphi_s(t) + \varphi_d(t) + \Gamma(t)\varphi_\Gamma$ which, upon differentiation, become

$$\partial\varphi/\partial t = (dU_x/dt)\varphi_0 + (dU_y/dt)\varphi_{90} + (d\Omega/dt)\varphi_\Omega + \partial\varphi_s/\partial t + \partial\varphi_d/\partial t + (d\Gamma/dt)\varphi_\Gamma \tag{21}$$

The first three terms are obtained once and for all; the last three are obtained at each time step. Consider these last three terms. From the definition of φ_s, given by Eq. (8), we have

$$\frac{\partial\varphi_s}{\partial t} = \frac{\partial}{dt}\int_w \gamma(c)G(r,t,c)dc \tag{22}$$

The potential φ_d is obtained by using the potential operator PO on $-\partial\varphi_s/\partial n$. Thus,

$$\frac{\partial\varphi_d}{\partial t} = \frac{\partial}{\partial t}\int_w \gamma(c)PO\left(\frac{-\partial G}{\partial n}\right)dc \tag{23}$$

Using Eqs. (22, 23, and 15) together gives

$$\frac{\partial(\varphi_s + \varphi_d + \Gamma\varphi_\Gamma)}{\partial t} = \frac{\partial}{\partial t}\int_w \gamma(c) \times \left[G + PO\left(-\frac{\partial G}{\partial n}\right) - \varphi_\Gamma\right]dc \tag{24}$$

Since the wake is growing, a term $\partial w/\partial t$ exists, and the time derivative of the integral is

$$\frac{\partial w}{\partial t}\left\{G(c_{TE}) + PO\left(-\frac{\partial G(c_{TE})}{\partial n}\right) - \varphi_\Gamma\right\}\gamma(c_{TE}) + \int_w \gamma\left\{\frac{\partial G}{\partial t} + PO\left(-\frac{\partial}{\partial t}\frac{\partial G}{\partial n}\right)\right\}dc$$

where c_{TE} is the end of the wake that is growing, i.e., at the airfoil trailing edge. Consider the term multiplying $\partial w/\partial t$. The term $G(c_{TE})$ is the potential due to a point vortex of unit strength located at the airfoil trailing edge. The disturbance potential $PO(-\partial G/\partial n)$ represents a flowfield that, when added to G, satisfies the boundary condition of no flow normal to the airfoil surface. If this point vortex, located on the exterior surface at the trailing edge, were moved a vanishingly short distance across the surface into the interior of the airfoil, a unit circulatory flow would result.§ Thus $G + PO(-\partial G/\partial n)$ is a unit circulatory flow equal to φ_Γ. The

§ See Ref. 8, p. 17.

term under consideration becomes $\partial w/\partial t(\varphi_\Gamma - \varphi_\Gamma)\gamma$, which is just 0. Equation (24) then reduces to

$$\frac{\partial(\varphi_s + \varphi_d + \Gamma\varphi_\Gamma)}{\partial t} = \int_w \gamma \left\{ \frac{\partial G}{\partial t} + PO\left(-\frac{\partial}{\partial n}\frac{\partial G}{\partial t} \right) \right\} dc \tag{25}$$

Since the wake is represented by a series of point vortices, the integral may be replaced by a sum over the number of vortices. The term $\partial G/\partial t$ is the time-rate-of-change of the potential due to a point vortex, and may be written as follows:

$$G(r,t,c) = Re\{(i/2\pi)\ln[\hat{r} - \hat{c}(t)]\} \tag{26a}$$

$$\partial G/\partial t = Re\{(i/2\pi)[(d\hat{c}/\partial t)/(\hat{r} - \hat{c})]\} \tag{26b}$$

where $\hat{r}$ and $\hat{c}$ are the complex coordinates of a general field point located at r and point vortex located at c in the wake, respectively, as viewed in airfoil coordinates. Here i is $(-1)^{1/2}$.

The forces and moments may be obtained easily by integrating the surface pressure directly. The pressure coefficient C_p, as well as the forces and moments, can be split into any number of additive parts. In particular, added-mass terms can be separated from circulatory terms if desired. In addition, the Lagally theorem can be applied, since we are dealing with source singularities on the body surface and vortex singularities in the wake.[13] Also, the Kirchhoff equation can be employed to obtain the added-mass forces and moments separately.[14] The Kirchhoff coefficients are calculated once and for all before the time loop is entered.

Gust

The gust, a special case, is discussed separately. The usual assumption that the airfoil does not affect the gust boundary is adopted. The velocity and potential field generated while the airfoil is traveling through the gust is calculated step by step in time, as V_d and φ_d were calculated. The gust itself may be thought of as an onset flow that causes a corresponding disturbance flow. The gust onset and disturbance flow must satisfy a homogeneous boundary condition on the airfoil surface, since fluid is not allowed to pass through the airfoil. If $\mathbf{V}_g(x, y, t)$ is the gust onset-flow velocity and if φ_g is the corresponding disturbance potential, the boundary condition for φ_g is

$$\frac{\partial\varphi_g}{\partial n} = \begin{cases} -\mathbf{V}_g\cdot\mathbf{n} & \text{on } S \text{ within gust} \\ 0 & \text{on } S \text{ out of gust} \end{cases} \tag{27}$$

The potential-flow operators PO and ∇PO are applied to $\partial\varphi_g/\partial n$ to produce the potential and velocity fields, respectively.

The potential φ_g is, of course, a function of time, since the boundary condition for φ_g changes as the airfoil passes through the gust and thus a contribution to the pressure through $\partial\varphi_g/\partial t$ is expected. If the onset gust field possesses a potential (call it φ_G), a contribution to the pressure from this potential is also expected. These contributions are

$$\partial\varphi_G/\partial t = \partial\varphi_G/\partial t + \mathbf{V}_s\cdot\nabla\varphi_G \tag{28a}$$

$$\partial\varphi_g/\partial t = PO(\partial^2\varphi_g/\partial t\partial n) \tag{28b}$$

The evaluation of $\partial\varphi_g/\partial t$ is a complex matter,[12] and only the final result for a sharp-edged gust of constant strength will be presented;

$$\partial\varphi_g/\partial t = \mathbf{V}_g\cdot\mathbf{n}\{F + PO(-\partial F/\partial n)\} \tag{29}$$

where F is the potential of unit point sources located at the points on the surface where the gust edge cuts the airfoil. For such a gust it is assumed that φ_G is also 0.

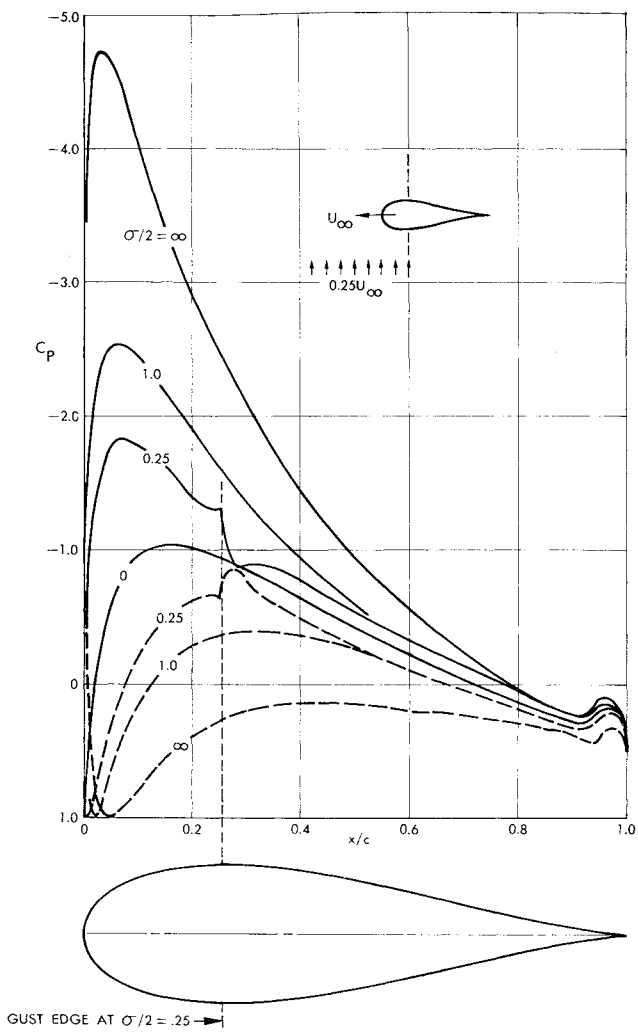

Fig. 3 Pressure distribution on a 25.5% thick Joukowski airfoil at various times before, during, and after its entrance into a sharp-edged gust.

Calculated Results

The present method can be used to calculate the pressures, forces, and moments on an airfoil of arbitrary shape moving along an arbitrary flight path. As was stated previously, the method is limited only by the storage of the computer that carries out the calculations. At present, the number of time steps is limited to 100 for the IBM 7094. The maximum number of coordinates used to describe the airfoil is also 100. A detailed computing-time study was not undertaken, but an approximate formula has been devised for a body that has 72 defining elements. This formula is

$$T(\text{min}) = 2.70(NT/20) + 5.15(NPT/20) + 1.0$$

where NT is the number of time steps taken, and NPT is the number of stations at which the pressure, forces, and moments are desired. For example, if $NT = 60$ and $NPT = 20$, the computing time is 14.25 min.

Two airfoils, an 8.4% thick, symmetric von Mises and a 25.5% thick, symmetric Joukowski, are used in most of the calculations and comparisons given. These airfoils were chosen only because experimental data and other theoretical analyses were available for them, not because they have simple, analytical shapes. An airfoil of any shape can be handled, since all that is required by way of input to the computer program are the coordinates of the airfoil and the flight-path time history. The flight path may be given as a tabulated set of airfoil positions and angular orientations, along with a table of time step intervals. As an option,

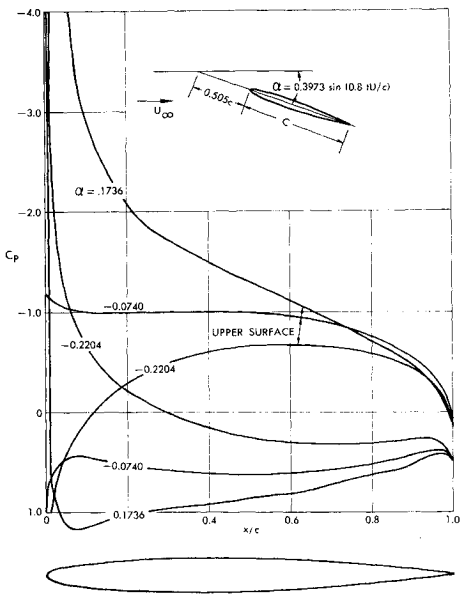

Fig. 4 Pressure distributions on an 8.4% thick von Mises airfoil, moving in a simple harmonic manner, at various angular positions.

built-in functions may be activated that generate the required time history data. If a gust is required, its edge and strength (vertical velocity) are input. At present, only a simple sharp-edged gust can be handled; however, the method is not limited to this case, and it is possible to extend the computer program to handle any type of gust.

The present method handles all problems as initial-value problems. If calculations are desired for airfoils operating in a periodic manner, all starting transients will be accounted for. If these transients are not desired, the calculations must proceed until the transients are sufficiently damped, which requires many time steps. Therefore, the method is particularly suitable for handling transient airfoil problems. Figure 3 shows the pressure distribution on a 25.5% thick, symmetric Joukowski airfoil at various stages as it passes through a gust.

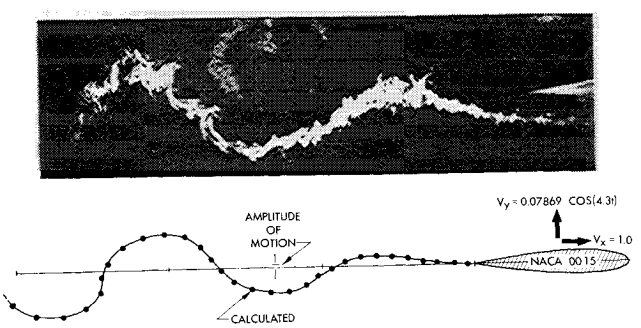

a) Frequency = $4.3U_\infty/c$

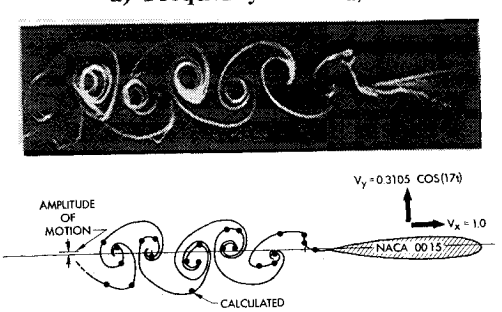

b) Frequency = $17.0U_\infty/c$

Fig. 5 Shape of the vortex wake generated by a NACA 0015 airfoil vibrating in a simple harmonic manner with an amplitude of 0.018c.

The first stage, $\sigma/2 = 0$, corresponds to the time before the airfoil enters the gust. The second stage, $1.0 > \sigma/2 > 0$, corresponds to the time when the gust edge is passing over the airfoil. In particular, the pressure distribution on the airfoil at the time when the gust edge is at the quarter-chord point is shown in the figure. The third stage shown occurs when the gust passes over the trailing edge; i.e., $\sigma/2 = 1.0$. The fourth stage corresponds to the airfoil at an infinite distance from the gust edge, $\sigma/2 = \infty$. Of particular interest is the irregularity in pressure at the points on the airfoil where the edge of the gust intersects the surface. At these points the pressure distribution possesses a logarithmic singularity. The strength of the singularity is slight, and, thus, the effect of the singularity is localized. Instead of a slender spike in the pressure, the average pressure over the element cut by the gust is given. The average can be obtained, since the singularity is integrable. The pressure distribution in the immediate vicinity of the trailing edge does not display the behavior characteristic of the Joukowski airfoil, because the trailing edge has been thickened slightly to increase the accuracy of the potential-flow calculations. This slight modification does not affect the pressures at other points on the airfoil surface.

Figure 4 shows the pressure distribution on an 8.4% thick, symmetrical von Mises airfoil as it undergoes periodic pitching and plunging. Several representative pressure distributions are shown. In this case, transient effects were not wanted and were eliminated by allowing the airfoil to move for a long interval of "time."

Figures 3 and 4 show the present method's capability of calculating pressure distributions. Also of interest are the trailing wake shapes generated by airfoils in transient and periodic motions, since it is the wake deformation that is the nonlinearity in the problem considered. For trailing-vortex wake shapes, Bratt[15] has obtained qualitative data in the form of smoke-trace photographs. A qualitative comparison of calculations by the present method with two of these smoke-trace photographs is shown in Figs. 5a and 5b. The calculated vortex sheets are represented by point vortices and the line faired through the points. In Figs. 5a and 5b, notice that the width of the wake, even as close as one chord length downstream, is 15 to 20 times as large as the amplitude of motion of the airfoil. This shows that the frequency as well as the amplitude of motion can generate large nonlinear effects. At high frequencies a vortex sheet of great strength is produced, leading to large deformations in the wake shape.

An exhaustive analysis of the accuracy of the wake-vortex-shape calculations has not been undertaken. Numerical solutions for wake shapes, and their corresponding accuracy, have been treated extensively by other authors, among them Rosenhead,[16] Fage and Johansen,[17] Hama and Burke,[18] and Birkhoff and Fischer.[19] It has been the experience of the author that sufficient accuracy has been achieved in the wake calculations to produce very good results for the pressure and force acting on the airfoil. Figure 6, for example, shows an airfoil that has started impulsively from rest at an extreme angle of attack. Numerical errors in the vortex-wake calculation would be expected to be at their largest in this case. The

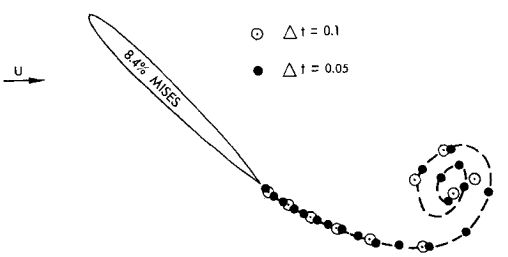

Fig. 6 Comparison of wake shapes calculated with two different time-step sizes.

shape of the wake generated by using two different time-step sizes is shown in this figure. In addition, the number of defining coordinates for the airfoil in the two cases is different. For the case $\Delta t = 0.05$, 95 coordinates are used to define the airfoil shape. For the case $\Delta t = 0.10$, only 73 coordinates are used. The difference between the two wake shapes is noticeable only in the rolled-up portion. This difference in wake shape has a negligible effect on the lift of the airfoil in the position shown. Specificially, the normalized lift values L/L_Q (L_Q is the quasi-steady lift) for the two cases are 0.5992 and 0.5995 for the airfoil in the position shown in Fig. 6.

Effects of Nonlinearity

Strictly speaking, all nonlinearities in the problem at hand arise from the wake; i.e., finding the wake shape involves a nonlinear process. However, if the boundary condition on the airfoil surface is not linearized, in one sense we may say that nonlinear effects also arise at the airfoil surface. The boundary condition on the airfoil surface is satisfied exactly by the present method, and, thus, "nonlinearities" arise from the airfoil shape.

The nonlinear effects of thickness and wake deformation on the Wagner, Küssner, and Theodorsen functions are discussed in the next three subsections. In all cases, the normalized lifts referred to are those due to the circulation and wake alone and do not include added-mass terms.

Wagner function

The Wagner function[3] is the time history of the normalized circulatory lift on an airfoil that has been started impulsively from rest at an angle of attack. This function is used to build up any kind of transient motion by simply considering the motion as a series of impulsive starts at various angles of attack. The motion is then obtained by using the superposition integral with the product of the Wagner function and the angle-of-attack function as the integrand.

Wagner obtained his function with the aid of linear theory. In particular, a flat plate at infinitesimal angle of attack was considered. The effect of airfoil thickness on the Wagner function is shown in Fig. 7a; that is, a comparison of the Wagner function for a flat plate with that obtained by the present method for a symmetric 8.4% thick von Mises airfoil and a symmetric 25.5% thick Joukowski airfoil is shown. The angle of attack for the airfoils is 0.01 rad; thus, nonlinearities due to wake deformation do not enter into the calculations of the present method. At such small angles of attack, the wake produced is too weak to deform to any noticeable degree. Figure 7a shows that the effect of airfoil thickness is to retard the build-up of lift; i.e., a thick airfoil takes longer to reach a given value of lift.

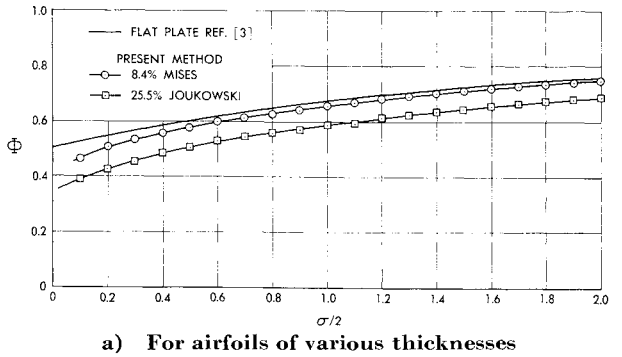

a) For airfoils of various thicknesses

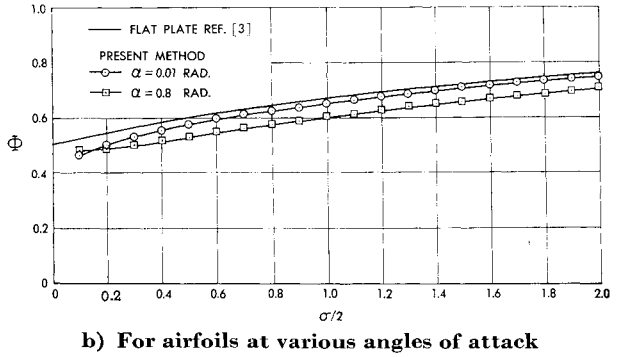

b) For airfoils at various angles of attack

Fig. 7 Comparison of calculated results with the Wagner function.

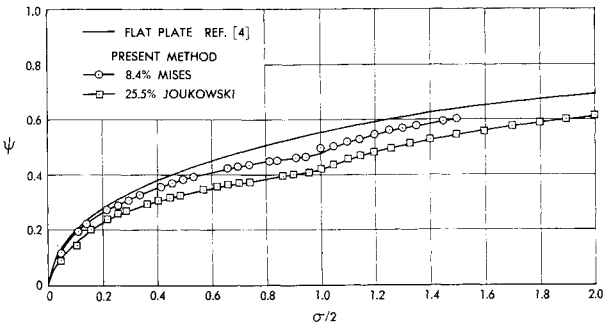

Fig. 8 Comparison of the Küssner function for airfoils of various thicknesses.

The effect of wake deformation on the Wagner function is also of interest. The effect of such deformation is similar to that of thickness, as Fig. 7b shows. In this figure, the effect of angle of attack on the Wagner function for the 8.4% thick von Mises airfoil is presented. Two angles of attack are considered, $\alpha = 0.01$ rad (no wake deformation) and $\alpha = 0.8$ rad. The wake shape at the time $t = U_\infty/c$ for the case $\alpha = 0.8$ is shown in Fig. 6. It must be stated that, once the wake is allowed to deform, the Wagner function as calculated by the present method cannot be used in the superposition integral. Figure 7b is only meant to indicate the region of validity of the linear Wagner function by showing the effects of wake deformation. However, the Wagner function that has been corrected for thickness can still be used in the superposition integral, since thickness is not a true nonlinearity.

Küssner function

Küssner[4] developed the function $\psi(\sigma)$, which can be used to find the lift acting on a flat plate entering into a vertical gust of arbitrary nonuniform strength. Again, the superposition integral must be used. The Küssner function was later generalized to include the case of a gust with a horizontal as well as a vertical component of velocity.[20] The linearized gust function $\psi(\sigma)$ represents the normalized lift that acts on a flat plate that is passing into a sharp-edged vertical gust of infinitesimal strength. Küssner derived the function with the assumption that the flat plate and its wake do not affect the gust boundary. This assumption was also made when the present method was applied to the problem. Figure 8 shows the effect of airfoil thickness on the Küssner function. This figure compares the Küssner function for a flat plate in a gust of infinitesimal strength with that obtained for an 8.4% thick von Mises airfoil and a 25.5% thick Joukowski airfoil entering a gust whose vertical velocity is 0.01 U_∞. The effect of thickness on the Küssner function is similar to the effect of thickness on the Wagner function. The nonlinear effect of the magnitude of the gust's vertical velocity has been studied. No appreciable effect on the Küssner function has been observed, even for a case where the vertical velocity of the gust is 0.5 U_∞. The wake deformations in the gust case happens to be small, even for large vertical gust velocities. The result is that the nonlinear effects on the lift are even smaller.

Theodorsen function

Theodorsen[2] and Karman and Sears[1] derived the function $C(k)$, which can be used, with aid of the superposition integral,

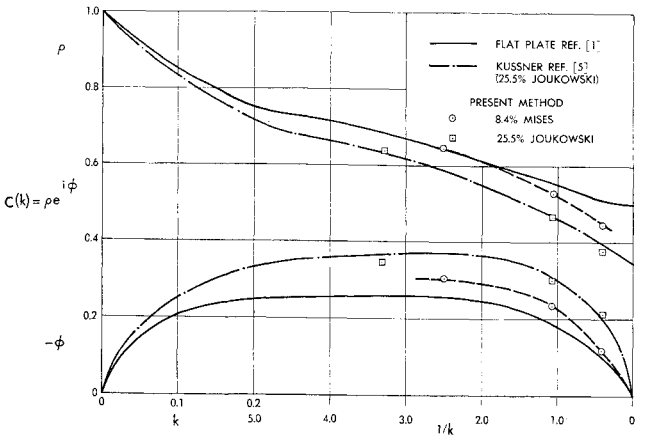

a) For airfoils of various thicknesses

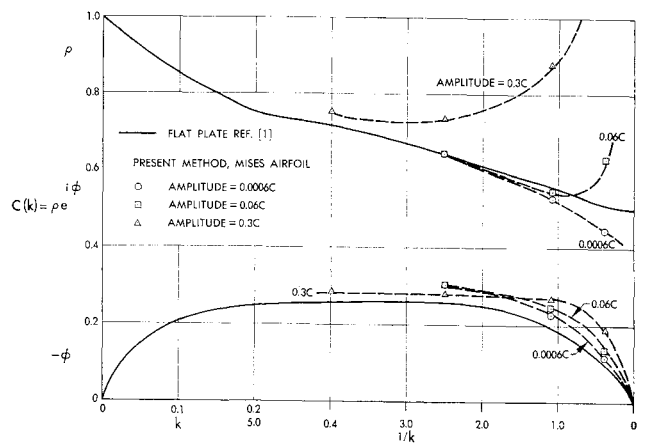

b) For airfoils oscillating at different amplitudes

Fig. 9 Comparison of calculated results with the Theodorsen function.

to find the lift on a flat plate executing arbitrary periodic motions of infinitesimal amplitude. The lift obtained in this manner is due to the circulation and wake flow alone, and thus the added-mass terms should be added to find the total lift. The Theodorsen function is time complex and is usually written as $F + iG$. In this paper it will be written in an alternate form, as $\rho e^{i\varphi}$, where $\rho = (F^2 + G^2)^{1/2}$ and $\varphi = \tan^{-1}(G/F)$. Specifically, the Theodorsen function is the normalized lift acting on a flat plate undergoing simple harmonic vibration. The term ρ, in the Theodorsen function, is the amplitude ratio, and $-\varphi$ the phase lag of the normalized lift.

The Theodorsen function cannot be obtained directly from the results of the present method. Since the present method is perfectly general, the values of lift obtained have harmonics of all orders. A Fourier analysis of the circulatory lift and the quasi-steady lift was made, to isolate the first harmonic. The first harmonic is, of course, much larger than any of the others. For instance, for the case of the von Mises airfoil oscillating with an amplitude of $0.3c$ and a frequency of $1.866\ U_\infty/c$ the third harmonic of the circulatory lift (which is next largest) is 6.7% of the first harmonic.

As was mentioned, Theodorsen obtained results for a flat plate. Figure 9a shows the effect of airfoil thickness on the Theodorsen function. It presents several values of the Theodorsen function for the symmetic 8.4% thick von Mises airfoil and the symmetric 2.5% thick Joukowski airfoil as obtained from results of the present method. The amplitudes of vibration at the quarter-chord points are $0.0006c$ and $0.0012c$, respectively. Since the amplitudes are so small, nonlinearities due to wake deformation do not appear. Also shown in the figure is the Theodorsen function for the flat plate and the Theodorsen function for the 25.5% thick Joukowski airfoil as given by Küssner.[5] The values obtained by using the present method for the Joukowski airfoil compare fairly well with Küssner's results. The general effect of thickness is to reduce the normalized lift for all frequencies and to increase the phase lag between the quasi-steady and total circulatory lift functions.

The effect of amplitude on the Theodorsen function, shown in Fig. 9b, is also of interest. In addition to the Theodorsen

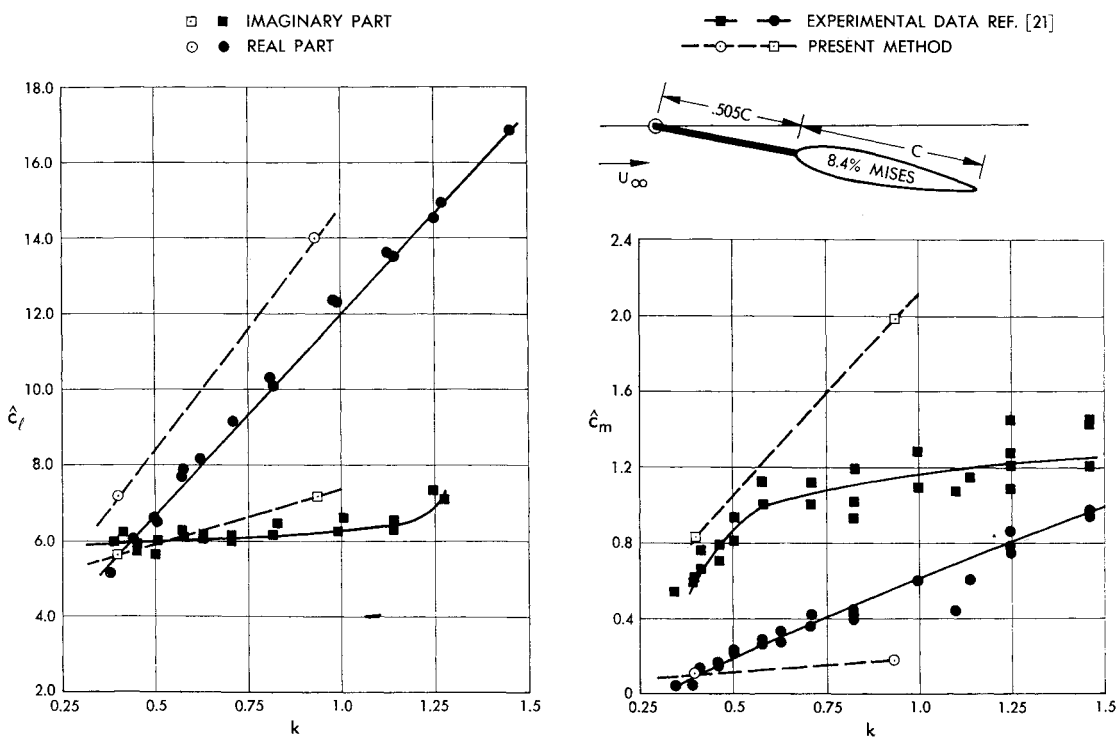

Fig. 10 Comparison of calculated and experimental reduced circulatory lift and moment coefficients for an airfoil oscillating in a simple harmonic manner with an amplitude of 0.06 c.

function for flat plates undergoing small-amplitude, simple harmonic motions, several values of the Theodorsen function for the 8.4% thick von Mises airfoil operating at several amplitudes are shown in this figure.

The amplitude of motion has a large effect on the Theodorsen function at high frequencies. This effect is opposite to the effect of thickness. The linear Theodorsen function can be obtained from the linear Wagner function by using the superposition integral. Therefore, one might expect the nonlinear effects for these two functions to be similar. Since the nonlinear effects act in the same direction as the thickness effects for the Wagner function, one might expect that the nonlinear effects might act in the same direction for the Theodorsen function. However, they do not. This result shows that the superposition integral cannot be used if a deforming wake is considered.

Added Mass

Heretofore, only the forces and moments acting on an airfoil due to the presence of a wake and circulation were considered for comparison. There are, of course, the added mass forces and moments that must be considered when total forces and moments are sought. The added-mass coefficients can be obtained by following Lamb [see Ref. 14, p. 164, Eq. (3)]. The added-mass coefficients obtained by the present method and those obtained by other methods (Küssner[5]) are in substantial agreement (see Ref. 12).

Experimental Comparisons

Spurk[21] has experimentally obtained the forces and moments acting on symmetrical von Mises and Joukowski airfoils. The airfoils were made to vibrate with small amplitude about an average angle of attack of zero. The airfoils were attached to rocker arms and made to oscillate about the hinge point of the rocker arm (see the drawing in Fig. 10). In this way the airfoils were given pitching as well as plunging motions. The experimental apparatus was designed in such a way that added-mass terms proportional to the airfoil accelerations were not measured. Unfortunately, not all of the added-mass terms were eliminated in this manner. Thus, the lift and moment obtained are not due entirely to the circulation and wake. The force and moment coefficients $\hat{C}_l$ and $\hat{C}_m$ are obtained from the measured data by dividing first by $\frac{1}{2}\rho U_\infty{}^2 c$ and then by the quarter-chord amplitude ratio h/c. A comparison of experimental data with calculated results for $\hat{C}_l$ and $\hat{C}_m$ is shown in Fig. 10. The airfoil considered is the 8.4% thick symmetric von Mises airfoil. The quarter-chord amplitude is 0.06 chord, and the angular displacement amplitude is 0.0796 rad. A similar comparison for the 25.5% thick Joukowski airfoil was made.[12] The present method and the experiment do not agree as well for the Joukowski airfoil as for the von Mises airfoil.

Since the present method is an exact potential-flow solution for the unsteady airfoil problem, any differences between its results and accurate experimental data must represent a failure of its mathematical model. Figure 10 shows that there is a difference between calculated results and experimental data. Even though viscosity is usually just a scapegoat for most discrepancies between aerodynamic theory and experiment, in this case the blame seems to be well-placed. An insight into the effect of viscosity on the Theodorsen function can be obtained if the experimental data are cast into the form of the Theodorsen function. This was done[12] with calculated values of L_Q. The conclusions that are drawn are summarized as follows: 1) the amplitude ratio, $\rho = L/L_Q$, is lower over the entire frequency range studied, and 2) the phase lag, $-\phi$, tends to increase rather than decrease in the high-frequency range. The low values of amplitude ratio may be due to the calculated quasi-steady lift L_Q which was too large. An experimental L_Q (which is not available) might bring it into line. The mechanism by which the viscosity modifies the phase shift is, however, still to be explained.

References

[1] von Karman, T. and Sears, W. R., "Airfoil Theory for Non-Uniform Motion," *Journal of the Aeronautical Sciences*, Vol. 5, No. 10, 1938.

[2] Theodorsen, T., "General Theory of Aerodynamic Instability and the Mechanism of Flutter," Rept. 496, 1940, NACA.

[3] Wagner, H., "Dynamischer Auftrieb von Tragflügeln," *Zeitschrift fuer Angewandte Mathematik und Mechanik*, Vol. 5, 1925, p. 17.

[4] Küssner, H. G., "Das zweidimensionale Problem der beliebig bewegten Tragfläche unter Berücksichtigung von Partialbewegungen der Flüssigkeit," *Luftfahrtforschung*, Vol. 17, 1940, p. 355.

[5] Küssner, H. G. and Gorup, G. V., "Instationäre linearisierte Theorie der Flügelprofile endlicher Dicke in kompressibler Strömung," *Mitteilungen des Max-Planck-Instituts für Strömungsforschung und der Aerodynamischen Versuchsanstalt*, No. 26, Göttingen, 1960.

[6] Van De Vooren, A. I. and Van De Vel, H., "Unsteady Profile Theory in Incompressible Flow," *Archiwum Mechaniki Stosowanej*, Vol. 3, No 16, 1964.

[7] Hewson-Browne, R. C., "The Oscillation of a Thick Aerofoil in an Incompressible Flow," *Mechanics and Applied Mathematics*, Vol. XVI, Feb. 1963.

[8] Smith, A. M. O. and Pierce, J., "Exact Solution of the Neumann Problem. Calculation of Non-Circulatory Plane and Axially Symmetric Flow about or within Arbitrary Boundaries," Rept. ES-26988, 1958, Douglas Aircraft Co.

[9] Hess, J. L. and Smith, A. M. O., "Calculation of Potential Flow about Arbitrary Bodies," *Progress in Aeronautical Sciences*, Vol. 8, Pergamon Press, Oxford, 1966, pp. 1–138.

[10] Giesing, J. P., "Potential Flow about Two-Dimensional Airfoils," Rept. LB 31946, 1965, Douglas Aircraft Co.

[11] Giesing, J. P., "Unsteady Two-Dimensional Potential Flow with Lift," Rept. LB 32144, 1965, Douglas Aircraft Co.

[12] Giesing, J. P., "Nonlinear Two-Dimensional Unsteady Potential Flow with Lift," Paper 66-968, Dec. 1966, AIAA.

[13] Milne-Thomson, L. M. *Theoretical Hydrodynamics*, Macmillan Co., New York, 1961.

[14] Lamb, H., *Hydrodynamics*, Cambridge University Press, 1932.

[15] Bratt, J. B., "Flow Patterns in the Wake of an Oscillating Airfoil," R & M 2773, 1953, Royal Aeronautical Establishment.

[16] Rosenhead, L., "Formation of Vortices from a Surface Discontinuity," *Proceedings of the Royal Society*, A134, 1931, p. 170.

[17] Fage, A. and Johansen, F. C., "The Structure of the Vortex Sheet," *Philosophical Magazine*, Vol. 5, 1928, p. 417.

[18] Hama, F. R. and Burke, E. R., "On the Rolling up of a Vortex Sheet," TN BN-220, 1960, University of Maryland.

[19] Birkhoff, G. D. and Fisher, J., "Do Vortex Sheets Roll Up?," *Rendiconti del Circolo Matematico Palermo*, Vol. 8, No. 1, 1959, p. 77.

[20] Drischler, J. A. and Diederich, F. W., "Lift and Moment Responses to Penetration of Sharp-Edged Traveling Gusts, with Application to Penetration of Weak Blast Waves," TN 3956, 1957, NACA.

[21] Spurck, J., "Measurements of the Aerodynamic Coefficients of Oscillating Airfoils in the Wind Tunnel and Comparison with Theory," Max Planck Institut, No. 29, Göttingen, 1963; also translation by G. de Montalvo, Rept. LB-31959, Nov. 15, 1964, Douglas Aircraft Co.